

FINAL PUBLISHABLE JRP REPORT

JRP-Contract number	NEW01	
JRP short name	TReND	
JRP full title	Traceable characterisation of nanostructured devices	
Version numbers of latest contracted Annex Ia and Annex Ib against which the assessment will be made	Annex Ia:	V1.1
	Annex Ib:	V1.1
Period covered (dates)	From 01 July 2012	To 30 June 2015
JRP-Coordinator	Alice Harling , National Physical Laboratory	
Name, title, organisation	Alice Harling , National Physical Laboratory	
Tel:	+44 (0)20 8943 7025	
Email:	Alice.Harling@npl.co.uk	
JRP website address	http://projects.npl.co.uk/NEW01-TReND/	
Other JRP-Partners		
Short name, country	BAM (Germany), CEA (France), CMI (Czech Republic), INRIM (Italy, PTB (Germany), ION-TOF (Germany),	
REG-Researcher (associated Home Organisation)	REG(CEA)	
Researcher name, title	Blanka Detlefs, Dr.	Start date: 01 Feb 2013
(Home organisation Short name, country)	(CEA, France)	Duration:12
REG-Researcher (associated Home Organisation)	REG(IMEC)	
Researcher name, title	Claudia Fleischmann, Dr.	Start date: 01 Feb 2013
(Home organisation Short name, country)	(IMEC, Belgium)	Duration:29

Report Status: PU Public

Issued: Sept 2015

Final Publishable JRP Version 1.0
Report

1 of 27

EMRP

European Metrology Research Programme
Programme of EURAMET



The EMRP is jointly funded by the EMRP participating countries within EURAMET and the European Union



TABLE OF CONTENTS

1	Executive Summary	3
2	Project context, rationale and objectives	3
3	Research results	5
4	Actual and potential impact	20
5	Website address and contact details	25
6	List of publications	25

1 Executive Summary

Introduction

This project has developed essential metrology for the chemical and electrical characterisation of novel materials and devices used in the micro and nano-electronic industry. The improvements in analytical capability gives the industry a set of reliable analytical methods to directly measure properties that determine device performance. This will underpin innovation of next generation electronics, provide valuable information for the optimisation of device manufacture and strengthen quality control.

The Problem

The micro and nano electronic world is experiencing a revolution in tackling the new challenges in terms of miniaturisation, power consumption, power density and processing speed. Novel inorganic semiconductor materials (Ge, InGaAs, GaN, SiC, and high-k dielectric materials) and novel 3D-architectures (Multiple Gates FETs, Nanowire T-FETs, etc.) with feature sizes < 30 nm are replacing traditional silicon devices. There is now a critical need for metrology to give traceable and quantitative chemical composition measurement of new inorganic electronic materials in complex 3D-architectures with buried interfaces and with nanometre depth resolution to enable the effective design and manufacture of such devices.

The Solution

An aim of the project was to reduce the relative uncertainties of analytical methods for the determination of surface contaminations, layer compositions and buried interface compositions of novel inorganic semiconductor materials. The non-destructive analytical methods of interest were Total Reflection X-Ray Fluorescence (TXRF) and Grazing Incidence X-Ray Fluorescence (GIXRF) analysis. In order to achieve reduced uncertainties, the partners optimised these analytical methods for the characterisation of nanolayered materials used in the development of nanoelectronic devices. Both the reliability and traceability of the applied methods were improved significantly, bringing relative uncertainties below 10 %. In particular, the accuracy of the x-ray standing wave field calculations was improved and validated.

The project has studied the effects of key parameters for argon cluster sputtering for depth profiling and 3D imaging of organic electronics materials and devices using secondary ion mass spectrometry (SIMS). The studies have led to an extensive description of argon cluster sputtering including a popular universal equation for the sputtered volume per ion dependence on the argon cluster energy, cluster size and incidence angle. The description provides a valuable basis for selecting appropriate experimental parameters for a given type of sample. The project has also established recommendations to reduce ion beam and electron beam damage effects in 3D imaging and sputter depth profiling to improve reliability of the analysis.

This project has demonstrated a novel method for 3D electrical characterisation of organic semiconductor nanostructures with resolution below 30 nm. The approach is based on the use of atomic force microscopy (AFM) and photoconductive AFM (PC-AFM) to map the local electrical and photo-electrical properties of organic semiconductor nanostructures. The project focused on two steps to achieve the objective, a) development of a reliable 2D mapping method, and b) development of a novel simulation tool to extract 3D nano-electrical information from the measurement data.

Impact

The project has delivered a high scientific output. To obtain a long term sustainable impact in the scientific community the communication channels of written manuscripts, presentations and training at conferences were chosen. The key data of the project are the following:

- 20 publications in the public domain and another 6 publications anticipated
- 66 conference presentations and posters
- 12 training sessions

The consortium organised several special sessions and workshops including a highly successful European Materials Research Society Symposium continuing the ALTECH conference series. In total 160 contributions were presented, including 11 invited presentations, 87 contributed oral presentations and 69 poster presentations.

Throughout the project, the partners engaged in pre-normative and standardisation activities in VAMAS (Versailles Project on Advanced Materials and Standards) and under ISO, as well as the national bodies DIN (Germany) and BSI (UK). Based on results from the project, NPL led the discussion on a standard for sputter depth profiling of organic materials at the ISO/TC201 (Surface Analysis) meeting in Berlin, September 2014. The development of a standard was encouraged by the committee.

2 Project context, rationale and objectives

2.1 Context

The micro and nano electronic world is experiencing a revolution in tackling the new challenges in terms of miniaturisation, power consumption, power density and processing speed. Novel inorganic semiconductor materials (Ge, InGaAs, GaN, SiC, and high-k dielectric materials) and novel 3D-architectures (Multiple Gates FETs, Nanowire T-FETs, etc.) with feature sizes < 30 nm are replacing traditional silicon devices. There is now a critical need for metrology to give traceable and quantitative chemical composition measurement of new inorganic electronic materials in complex 3D-architectures with buried interfaces and with nanometre depth resolution to enable the effective design and manufacture of such devices.

Concurrent with these developments is the emergence of electronics based on organic semiconductors, made of small organic molecules or conductive polymers arranged in ordered assemblies. This is an important new knowledge-based, high innovation and high value (multibillion €) sector for the EU. Unfortunately, the techniques developed for the inorganic semiconductor industry do not directly apply and there is an urgent need for methods to give 3D nanoscale chemical and electrical imaging. For organic electronic materials, the state of the art for chemical imaging at the outset of the project, 3D SIMS with C₆₀ sputtering, failed completely and no methods were available for 3D nanoscale electrical measurements where a resolution better than 30 nm is needed. The challenges are for metrology at the nanoscale and it is clear that no single technique can provide all the answers required by industry. Whilst a single technique may offer repeatable high precision results, the accuracy (closeness to a true value) of all techniques is limited. This causes major difficulties in manufacturing and research and development since a complete nanoscale picture cannot be reliably assembled. The solution is traceability of the nanoscale measurements and availability of nanostructured reference materials.

2.2 Objectives

The TReND project, "Traceable characterisation of nanostructured devices", aimed to address the micro and nano-electronic industry's needs for advanced measurement capability. Three scientific and technical objectives were defined for the project:

1. Improvement of non-destructive methods for the characterisation of nanolayers and buried interfaces, by chemical depth-profiling of nanolayers (up to 200 nm) with trace level sensitivity.

This objective was to support the development and implementation of novel nanolayered materials, including organic and inorganic thin films for new semiconductor devices. Within the project a strong focus was set to qualify complementary analytical techniques to provide reliable quantification of the composition of beyond state-of-the-art materials for next generation devices. Grazing-incidence X-Ray Fluorescence (GIXRF) in combination with X-ray Absorption Fine Structure (XAFS) analysis were identified to hold potential for providing high sensitivity analysis of surface and buried interface contamination, as well as elemental depth-profiling capabilities with high information depths up to 200 nm. However, a strong collaborative effort of all partners was required to realise this potential to achieve traceable non-destructive measurements. The specific requirements for that, which have been successfully provided by the project, were access to beyond state-of-the-art samples, validated and optimised x-ray spectrometric techniques, improved depth-profiling capabilities of GIXRF, a new method combining GIXRF and XAFS to characterise OPV devices and reduced relative uncertainties of the quantification.

2. Development of essential metrology to enable 3D nanoscale chemical imaging of organic electronic materials using secondary ion mass spectrometry with new massive argon cluster sputtering.

3D molecular imaging using secondary ion mass spectrometry (SIMS) with sputtering by novel argon clusters gives new capability for chemical imaging and depth profiling of organic electronic devices. This holds the potential for measuring the chemical composition in 3D and revealing the presence of artefacts or contaminants in the devices. Such information is highly valuable in the R&D of organic electronic devices. Argon cluster ion sources became commercially available around 2011 – 2012. However, the understanding of argon cluster sputtering at that time was poor and a detailed investigation of physical parameters was needed to identify operating conditions for optimal analytical capability and reliability. Additionally, there was very little published data on the matrix effects that affect quantification in depth profiling and no reports on the effects at interfaces. In manufacturing organic electronic devices, an important issue is the effect of migration of high mobility inorganic species from the cathode into the organic layer reducing device efficiency and lifetime. Methods were required to measure this.

3. Development of a novel method for 3D nano scale electrical characterisation of organic electronic materials (with resolution better than 30 nm) and nanostructured self-assembled reference materials for the metrological studies of the techniques.

Prior to this project, mapping of surface and near-surface currents at the nano-scale was at a proof-of-concept stage. Such information is highly valuable for the intelligent design of new nanoscale based (opto)electronic devices. Photoconductive AFM (PC-AFM) had been found to show great promise as a novel technique for this purpose with a potential lateral resolution of 30 nm. However, the quantification of signals coming from the depth of the sample depends on material properties. A significant effort was required to improve the understanding of this, as well as the reliability of the method. To support the metrology studies there was a need for appropriate optoelectronic reference samples with well-known nanoscale morphology.

3 Research results

The project was organised in three technical work-packages, each addressing one of the technical and scientific objectives.

- 1) Traceable chemical and elemental depth characterisation of inorganic nanolayers and buried interfaces
- 2) 3D nanoscale imaging of organic electronic materials
- 3) 3D nano-electrical and optical characterisation of organic semiconductor nanostructures.

The results from the technical work are reported below.

3.1 Traceable chemical and elemental depth characterisation of inorganic nanolayers and buried interfaces

Throughout the project, relevant material systems were identified and fabricated at the Research Excellent Grant Home Organisations to support the experimental work. Both Research Excellent Grant researchers (REGs) at CEA and IMEC provided various semiconductor materials to the other partners for the development and further optimisation of the x-ray spectrometric techniques, and also provided complementary analysis of the materials. Of particular interest were samples with new nanolayered materials beyond the state-of-the-art. Examples are new high-k materials, materials with designed electrical properties such as nano-laminates and new organic materials for photovoltaic devices.

The collaboration of the metrology institutes and the REG researcher at the semiconductor R&D institutes REG(IMEC) and REG(CEA) was essential to successfully develop and apply new metrology as it is required to enable faster progress in the design and fabrication of improved semiconductor devices.

An aim of the project was to reduce the relative uncertainties of analytical methods for the determination of surface contaminations, layer compositions and buried interface compositions of novel semiconductor materials. The analytical methods of interest were Total Reflection X-Ray Fluorescence (TXRF) and Grazing Incidence X-Ray Fluorescence (GIXRF) analysis. In order to achieve reduced uncertainties, the partners involved optimised these analytical methods for the characterisation of novel nanolayered materials originating from current material development for improved nanoelectronic devices. Both the reliability and traceability of the applied methods could be improved significantly. In particular, the accuracy of the x-ray standing wave field calculations could be improved and validated.

The most successful example for an improved analysis of novel semiconductor material was the characterization of high-k nanolayers by GIXRF. This was enabled by the strong cooperation of PTB and the two REGs at IMEC and CEA. In particular, the provision of beyond state-of-the-art materials was essential for PTB to optimize the analytical techniques and demonstrate the improved metrological capabilities. The results were published in the special issue on "High-k Materials and Devices 2014" of the peer-reviewed open-access journal *Materials* ([10] Müller et al., 2014).

The main achievements are:

- Optimized GIXRF excitation conditions for semiconductor materials.
- Improved spectral deconvolution of overlapping lines with reduced uncertainty of 2.5 %.
- Validated X-ray standing wave (XSW) field calculations.
- A reliable quantification of novel nanolayered materials without calibration samples or reference materials.

3.1.1 Optimization of the excitation conditions and the spectral deconvolution

Reliable determination of count rates from GIXRF spectra of samples with complex layer structures is often affected by overlapping fluorescence lines. In particular, the presence of intense L-line series can make determination of weak signals from thin layers or ultra-low contaminations ambiguous. In the case of semiconductor materials, the interfering L-line series often originate from III-V substrates or layers. An example is shown in Figure 1. The spectrum was recorded from a very thin high-k stack which was deposited on a 300 nm thick InGaAs layer on an InP substrate. Three L-series are visible in the spectrum, As and Ga L-lines around 1.1 keV to 1.3 keV as well as the L-lines of the heavier In between 3 keV and 4.3 keV. The In lines are overlapping strongly with the Al and Sc K-lines which are essential for the quantification of the Al₂O₃ and the Sc₂O₃ layer mass deposition.

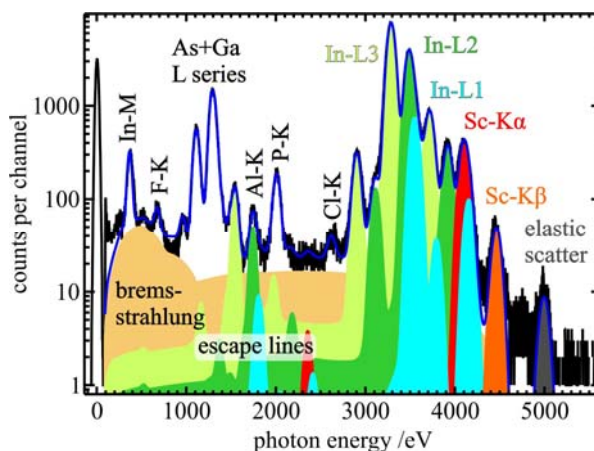


Figure 1: Deconvolution of a GIXRF spectrum recorded from a thin Sc₂O₃ layer buried under a thin Al₂O₃ layer. The sample was excited by a 5 keV x-ray beam under a grazing incident angle of 0.5°

To enable reliable determination of all lines in the spectrum the project took advantage of the tunability of synchrotron radiation selective excitation of the different absorption edges. The deconvolution of all spectra was performed by fitting a model spectrum employing the detector response functions. In case of the spectrum above the Sc K-edge all indium fluorescence line series were fitted using constant line sets for each sub shell (plotted in light green, green and cyan in Figure 1). In case of the spectrum above the Al K-edge the In L-series was not excited and no overlapping with Al K-line occurs.

This approach ensures an increased reliability of the determined count rates which reduces the relative uncertainties of the quantification to 2.5 %. Without the optimization, the determined Sc count rate would be affected by the overlapping In L1 lines causing a 10 % uncertainty contribution. The Al K-line is overlapped by the In L2 escape line which can cause a 50 % contribution. The method can also be used to reduce uncertainty for other relevant materials.

A systematic study comparing calculated XSW field intensity enhancements with measured GIXRF signals was performed using nanolayered materials with different layers and varying layer thickness to validate the X-ray standing wave (XSW) field calculations. An example of such a comparison is shown in Figure 2. The results show that the XSW field calculations are in good agreement with the measurements if the incident angle is above 0.3°. For very shallow angles large deviations were found. The reliability of the GIXRF quantification of thin layers is not affected by this because of the sufficiently good signal to noise ratio above 0.3°.

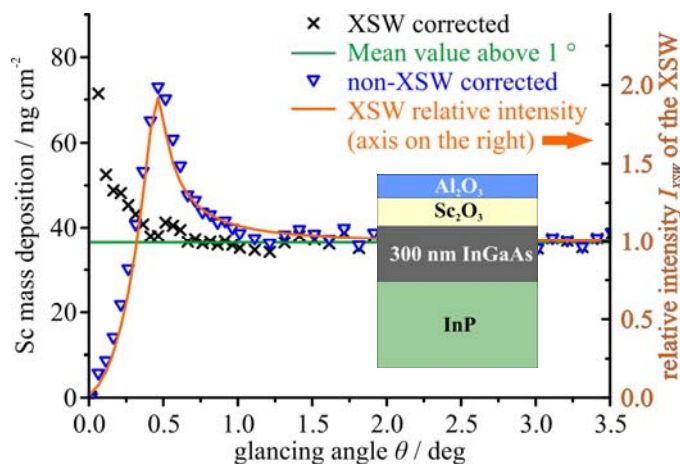


Figure 2: Determined Sc mass depositions plotted over the grazing incident angle with (black) and without (blue) taking into account the angular dependent x-ray standing wave (XSW) field intensity. Inset: Novel semiconductor materials quantified by GIXRF. The thickness of the Al₂O₃ and the Sc₂O₃ layer is in sub-nanometer range.

3.1.2 Improved elemental depth profiling for a limited selection of materials

To improve the grazing incidence X-ray fluorescence (GIXRF) based method for elemental depth profiling, methodologies were developed to incorporate X-ray reflectivity (XRR) both in the experimental and the data modelling part. XRR provides an experimental access to the optical constants of the sample under investigation. This is essential for correct modelling of the X-ray standing wave (XSW) field, which serves as the depth sensor in GIXRF-based depth profiling.

Using the experimental chamber for combined XRR and XRF experiments, both methods can be applied in parallel and no additional experiments are necessary. This ensures that both X-ray methods investigate an identical region of the sample, which is crucial if non-homogeneous or laterally structured samples are under study.

On the data modelling side, an iterative modelling approach, taking into account both the GIXRF and the XRR data was developed and applied to the depth profiles of ultra-shallow ion implants and the depth dependent compositional analysis of atomic layer deposited nanolayer stacks.

For the implant samples, the measured XRR is modelled using a simple layer stack consisting of e.g. SiO₂, amorphous Si and a silicon substrate. The fitting parameters for this model are the thicknesses of SiO₂ and a-Si, the optical constants n and k for SiO₂, a-Si and Si as well as a roughness σ , which is expected to be equal at each interface. The intensity distribution of the XSW as a function of the incident angle θ and the depth d is then calculated using the same layer stack with the XRR determined parameters. With the help of this calculation, an initial elemental depth profile for the implant is determined.

This initial depth profile is then used to derive a depth dependent modification of the optical constants of the substrate (usually a layer stack of SiO₂, amorphous Si and a silicon substrate) in the implanted depth region by mixing the substrate materials tabulated optical constants with the implants values according to the derived local concentration of the implanted element. The resulting depth profiles for n and k are then split up into sub layers and a new XSW field is calculated using this modified layer stack. In Figure 3, calculated depth profiles for σ and β using an initial fit for the B depth profile of a 1.05 keV BF₃ plasma immersion implantation with a nominal dose of 10¹⁵ At./cm² are shown. In the depth regime between 1 and 8 nm, the local values for the optical constants are modified due to the implanted boron. The step-change at 2 nm is due to the transition from SiO₂ to amorphous Si. The final depth profile is then determined using this modified XSW field distribution.

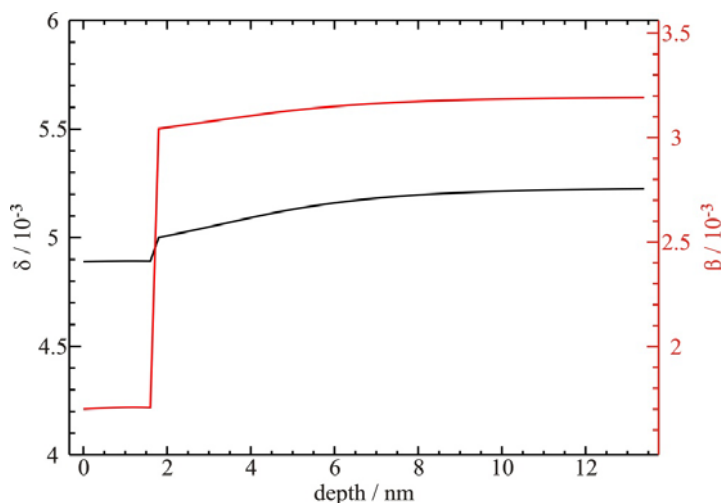


Figure 3: Depth dependent calculations for the optical constants σ and β using an initial fit for the B depth profile of a 1.05 keV BF_3 plasma immersion implantation with a nominal dose of 10^{15} At./ cm^2 .

For nanolayered samples, e.g. the investigated nano-laminate stacks consisting of thin $\text{Al}_2\text{O}_3/\text{HfO}_2$ layers, it is much more crucial to have access to the sample specific optical constants. The reason for this is that materials with thicknesses in the nm range are known to have densities, and thus optical constants, deviating from tabulated bulk data by up to 30%. A GIXRF depth profiling would therefore not be possible if only tabulated bulk optical constant data is available for the XSW field calculation. This is demonstrated in Figure 4 where an XRR curve, calculated using tabulated optical constants, is compared to a fit to the measured XRR optimizing only the optical constants. On the right hand side, the ratio of two XSW field distributions based on these two sets for the optical constants is shown. The deviations of more than 10 % do not allow for a reliable depth profiling based on the bulk optical constants.

In order to overcome this, a fitting routine for the full experimental data set (XRR and GIXRF) of each sample was developed. It simulates both the XRR and the GIXRF measurements for each sample using one layer model including intermixing between the layers. The fitting parameters within this model include the densities of each layer or material respectively, the degree of intermixing between two layers, the optical constants of each material as well as the roughness of the substrate.

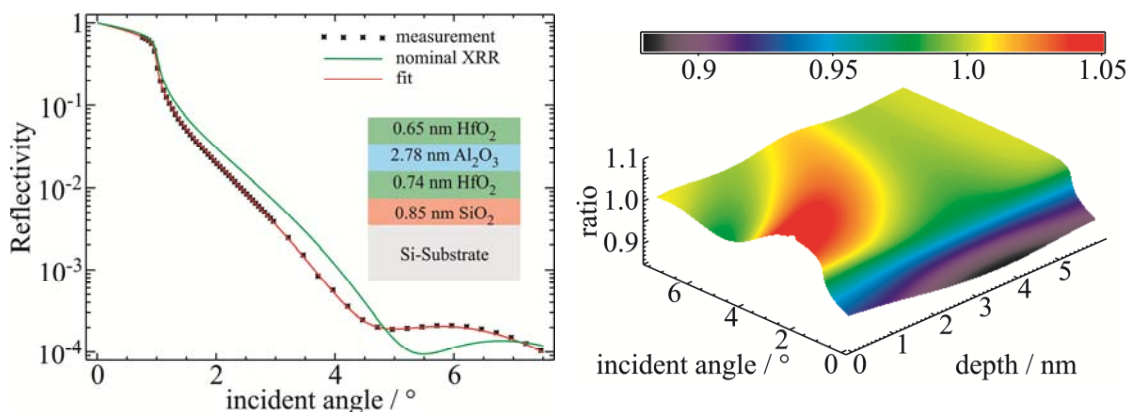


Figure 4: On the left hand side, a comparison of a calculated XRR curve using tabulated optical constants for the sample shown in the inset and a fit to the measured XRR optimizing only the optical constants is shown. The incident photon energy was 1622 eV. On the right hand side, the ratio of the two XSW fields, which correspond to the two XRR curves is shown.

A resulting depth profile of the material concentrations for one of the investigated $\text{Al}_2\text{O}_3/\text{HfO}_2/\text{Al}_2\text{O}_3$ layer stacks on silicon is shown Figure 5. Here, the parameter describing the width of the intermixing region was defined to be equal for all interfaces. An additional surface layer, to take into account contamination as well as x-ray induced carbon deposition during the measurements, had to be introduced. Parts of the work on this topic was published in a contribution entitled “Reference-free, depth-dependent characterization of nanolayers and gradient systems with advanced grazing incidence X-ray fluorescence analysis” to the journal *Physica Status Solidi A* ([13] Hönicke et al., 2015).

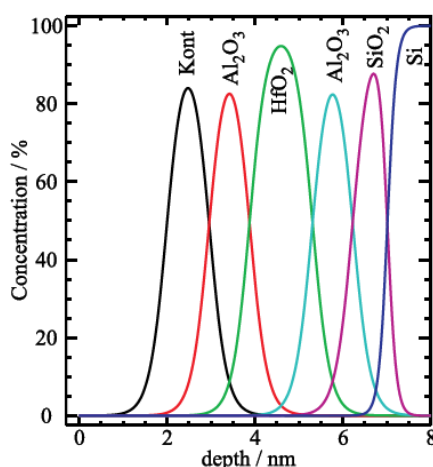


Figure 5: Resulting depth profiles for an $\text{Al}_2\text{O}_3/\text{HfO}_2/\text{Al}_2\text{O}_3$ layer stack on silicon with a native oxide layer.

3.1.3 Chemical speciation and phase identification of physical location of surfaces, buried nanolayers and interfaces

To identify chemical species at surfaces and interfaces in buried nanolayers, a new methodology combining grazing incidence geometry with near edge x-ray absorption fine structure spectrometry (NEXAFS), extended x-ray absorption fine structure spectroscopy (EXAFS) and diffractometry was developed by PTB, CEA, REG(imec) and REG(CEA). Furthermore the collaboration has demonstrated the capabilities of the combined method by the characterization of selected semiconductor materials, such as TiO_2 , Al_2O_3 , GdAlO_x , SnO_2 , beta-Sn, S, CuSO_4 ultra-thin films on various substrates.

The focus of these activities was on organic photovoltaic (OPV) materials and the respective devices. For these materials the combination of GIXRF and NEXAFS was most promising. The measured samples range from reference samples used for obtaining NEXAFS fingerprint spectra to complete device structures including front and backside electrodes. The layer structure of the OPV devices was a complex mixture of organic and inorganic nanolayers. The substrate was typically glass coated with an ITO layer as front contact. The active OPV film was usually 100 to 200 nm thick and consisted of a mixture of different organic molecules such as PCDTBT, a conjugated polymer, and PC_{70}BM , a fullerene derivative. The back contact was usually a thin Ag electrode layer placed at the top of the sample during the GIXRF-NEXAFS measurements. In addition, different oxide nanolayers were deposited as barrier layers between the organic film and the metal electrodes.

The major outcome of this task is a protocol which defines suitable methods (experimental parameters, reference materials, etc.) for the characterization of chemical composition, and chemical state as well as crystalline structure of organic photovoltaic (OPV) and inorganic semiconductor materials by a combined GIXRF-NEXAFS methodology. In addition, the general capabilities and limitation of the combined methodology have been investigated.

It was demonstrated that a depth-sensitive compositional analysis of OPV devices is feasible based on carbon K-edge spectra as long as radiation damage is prevented and proper reference materials are

available. Sulfur K-edge spectra reveal complementary information on the donor materials (polymer). In Figure 6, two NEXAFS spectra with a sensitivity tuned to different depths by choosing the appropriate grazing angle of incidence are shown. The high information depth obtained with NEXAFS in fluorescence yield mode allows for probing bulk properties of (buried) photoactive layers. The technique developed in this task was found to be ideally suited to study OPV cells that resemble a real device architecture and hence to complement electrical data.

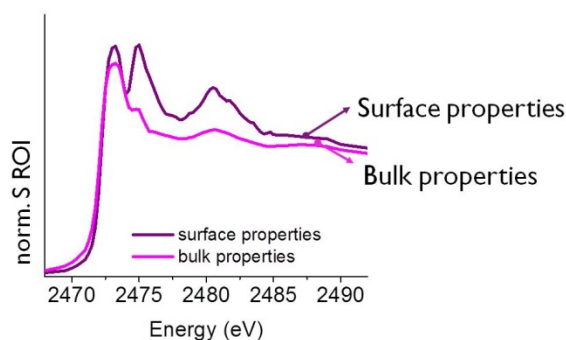


Figure 6: NEXAFS spectra of a thin P3HT film measured at the sulfur K-absorption edge. The surface sensitive and bulk sensitive spectrum have been recorded at grazing incident angles below and above the critical angle of total reflection respectively.

3.1.4 Traceable measurements of atomic fundamental parameters to improve the accuracy x-ray analytical methods

A final aim of this project was to measure relevant atomic fundamental parameter (FP) values. The parameters of interest were selected based on the chemical elements used in the nanostructured devices investigated in the project. The fundamental parameters include mass attenuation coefficients for Ti and Ta in the photon energy range between 100 eV – 30 keV for Ti and 2 keV – 35 keV for Ta and the fluorescence yield as well as the transition probabilities for the K-shell of Ti. The experiments were carried out at the BESSY II synchrotron by PTB and at the SOLEIL synchrotron by CEA. A set of samples were provided by BAM.

The experimental procedure to determine mass attenuation coefficients is by measuring the transmission of a free standing thin foil sample of the element of interest at the photon energy of interest. The transmission data can then be used to calculate the energy dependent attenuation and the mass attenuation coefficient can be calculated if the mass per area of the sample is known. The mass per area of the thin foil used at CEA was determined with high accuracy by measuring the area with a vision machine and measuring its mass with a weighing machine. Using this value, the thickness of the Ti foils used at PTB was calculated by fitting them to the CEA data in overlapping regions.

At the synchrotron source SOLEIL, the transmission experiments were conducted at the “Metrologie” beamline using the hard X-ray branch for energies above 3 keV and the XUV branch below 1.9 keV. PTB conducted the experiments at the PGM and FCM beamlines within the PTB laboratory at BESSY II.

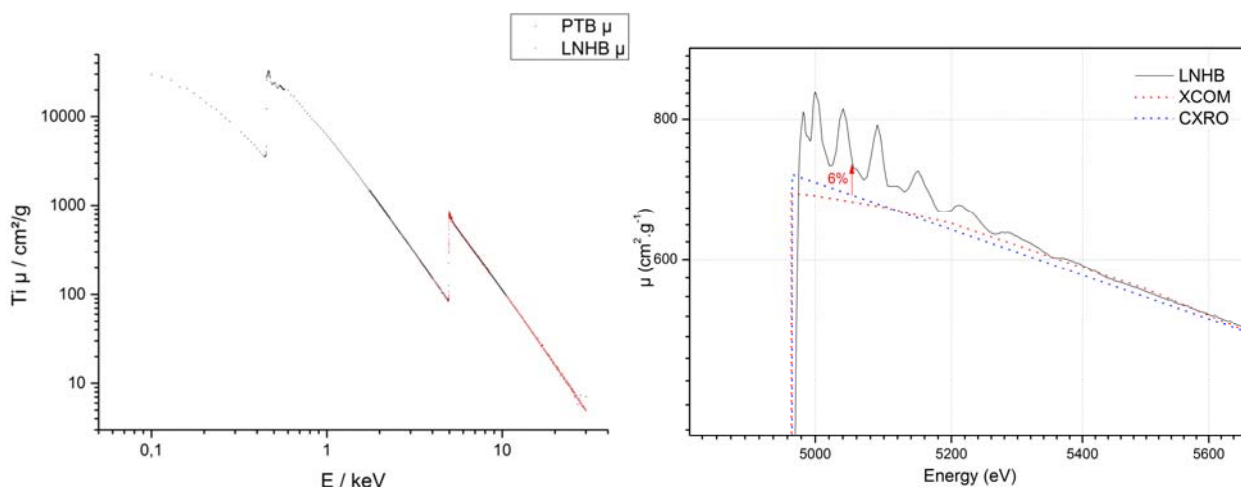


Figure 7: The determined mass absorption coefficients for Ti. On the right hand side, a detailed view of the determined mass absorption coefficients for Ti above K-edge (solid line), in comparison with data from the literature is shown.

In addition, PTB experimentally determined the fluorescence yield and the transition probabilities for the Ti-K shell by using PTBs reference-free X-ray fluorescence setup. By combining transmission and fluorescence experiments and due to the usage of calibrated instrumentation, e.g. calibrated photodiodes, the K-shell fluorescence yield can be calculated from the detected Ti-K fluorescence intensities. The determined value for Ti-K of 0.236 ± 0.008 is well in line with recent literature data and has a significantly reduced relative uncertainty of 3.5%. These results were published in a contribution entitled “Fundamental parameters of Zr and Ti for a reliable quantitative X-ray fluorescence analysis” to the X-ray Spectrometry journal ([17] Kolbe & Hönicke, 2015).

Table 1: The determined fluorescence yield for the Ti-K shell in comparison to literature data

	ω_K
This work	0.236 ± 0.008
Krause	0.218 ± 0.011
Bambynek	0.219 ± 0.018
Cullen	0.214
McGuire	0.233
Bhan	0.216
Bailey	0.221 ± 0.012
Han	0.234 ± 0.019
Ménesguen	0.23 ± 0.028

The FP data, which was determined within the project will substantially improve the reliability of the X-ray based characterisation methods and will allow for reduced relative uncertainties of the analytical results.

3.2 3D nanoscale imaging of organic electronic materials

Secondary ion mass spectrometry (SIMS) brings the power of mass spectrometry to the analysis of surfaces and provides valuable information for the development and innovation of new devices, materials and processes. The project's second work objective was to establish the essential metrology for 3D SIMS imaging of organics using large argon cluster sputtering.

The underlying process of SIMS is sputtering; a beam of energetic ions bombards the target and causes ejection of particles from the top few nanometers of the surface. Ionised ejected particles, the secondary ions, are identified using a mass analyser to reveal the chemistry of the surface. To create chemical maps of the surface, the ion beam is scanned across the sample surface to analyse point-by-point. This can be extended to depth resolved and 3D imaging by using a cluster ion sputter source to expose deeper layers of the material which can then be imaged. The primary ion source used for SIMS and the sputter ion source can be the same, but often two different ion sources are used as a good imaging ion source is not necessarily a good sputter ion source and *vice versa*. This is in particular true for the analysis of organics.

At the onset of the project, C_{60} was the most widely used ion source for sputter depth profiling of organic materials. This worked for some organic materials but failed completely for other classes of materials, including those used in the organic electronics industry, due to ion-induced chemical degradation of the exposed surface. A promising solution to this problem was offered with the introduction of large argon cluster ion beams. These cluster ions, consisting of hundreds or thousands of argon atoms, had been shown to permit sputtering of organic materials and expose a surface where the sample chemistry is maintained. In this project the effects of key parameters for argon cluster sputtering were studied, and the many outcomes provide a solid metrological foundation for optimal sputter depth profiling of organic electronic materials, and organic materials in general, with minimal chemical degradation and depth resolutions close to 5 nm. The objective of developing the essential metrology for argon cluster sputtering has firmly been achieved.

3.2.1 The effects of the argon cluster energy and the cluster size

Of particular interest are the argon cluster energy, E , typically between 2.5 keV and 20 keV, and the cluster size, n , typically between 250 and 5000 atoms. These largely govern the sputtering process and are the parameters that analysts can control. To develop an analytical model describing the effect of argon cluster

size on the sputtering yield, i.e. the number of atoms removed by each ion, measurements of the sputtering yields of gold using argon cluster ion beams of energies 5, 10 and 20 keV with $100 < n < 5000$ were made by NPL. The sputtering yield, Y , is important as this relates the current of the ion beam to the sputtered depth. This was found to exhibit a consistent dependence of Y/n on E/n for all beam energies showing that their effects are linearly additive in this regime, i.e. doubling the number of atoms in the cluster at the same energy per atom doubles the total yield. The work was reported in J. Phys. Chem. C ([1] Yang et al., 2012),

The sputtering yields for three organic materials, Irganox 1010, NPB and Irganox 3114, were also measured by NPL. The sputtering yields of organic materials are 2-3 orders of magnitude higher than those for gold. Yet, the sputtering yields, and data for other materials either provided by project partner ION-TOF or available in the scientific literature, showed a consistent dependence on E/n described by a simple universal equation

$$Y/n = B (E/An)^q / [1 + (E/An)^{q-1}]$$

In the universal equation, the parameters A , B and q are established by fitting. This universal equation exhibits no threshold energy, contrary to a popular understanding prior to this work. The parameter A is related to the mean energy per atom to release a fragment. This value is in the order of a few eV for organics and >50 eV for inorganics, the low value for organics being indicative of high sputtering yields. For materials with low A values, the universal equation in the energy range of interest is close to a linear dependence on energy. The difference between organic and inorganic materials is evident in Figure 8 which shows the sputtering yield dependence, as described by the universal equation, for a number of materials. This semi-empirical equation, which was published by NPL in J. Phys. Chem. C ([3] Seah, 2013), provides the basis for a descriptive model for argon cluster sputtering and has rapidly been taken up by the scientific community upon publication. For analysts, the equation is a useful guide when selecting E and n for the analysis of a particular sample.

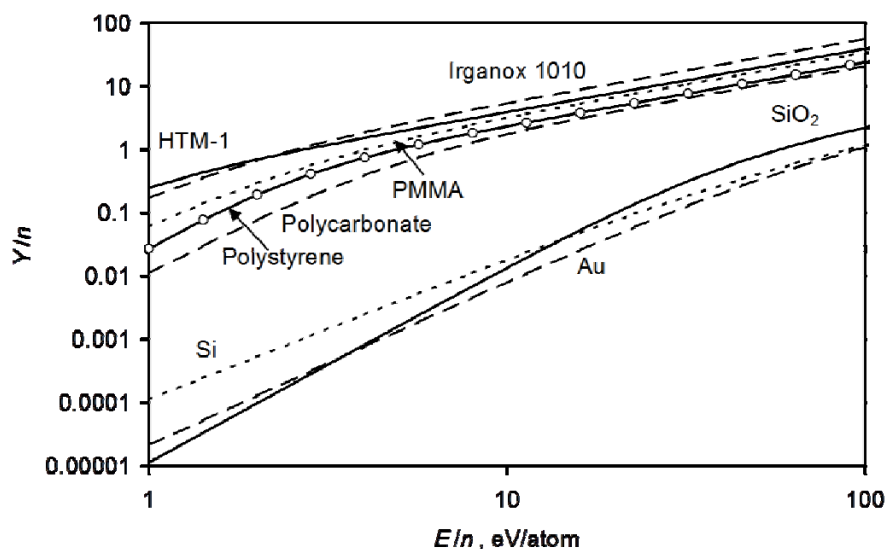


Figure 8: Universal equation fits for the sputtering yield per atom in the incoming argon cluster as a function of energy per atom in the argon cluster for a range of materials (From 3).

For the three organic materials mentioned above, Irganox 1010, NPB and Irganox 3114, the damage induced by the argon cluster ion beam was measured for ion beams with different energies and cluster sizes. The induced damage was shown to increase with increasing E/n . For NPB, a compound used in organic electronic displays, the dependence was critical and it was found that for successful, low damage, depth profiling $E/n \leq 10$ eV was required.

Typically, SIMS analysis of organics is conducted using a beam of small metal cluster ions, such as Bi_3^+ and Au_3^+ , as the primary ion beam. These have high secondary ion yields but also give complex spectra with a

high number of non-specific peaks arising from fragments of the sample's molecular constituents. SIMS can be conducted using an argon cluster beam as the primary ion beam. In that case the resulting mass spectrum depends on the cluster energy and the number of atoms in the cluster. NPL studied this for thin films of three compounds, Irganox 1010, fmoc-pentafluoro-L-phenylalanine, and NPB. The argon cluster mass spectra from these materials were generally simpler than those obtained with Bi_3^+ . It was found that decreasing E/n reduces the total ion yield but importantly also the relative abundance of peaks related to non-specific fragment ions. The E and n dependences for the separate fragments as well as the total ion yield were shown to be consistent with the universal equation above. From this theory, conditions for the highest yields of characteristic fragments for imaging or whole molecular ions for identification from any organic compound are readily defined and optimisation of instrumental operating conditions easily identified. The work was published in J. Phys. Chem. C ([9] Seah et al., 2014).

3.2.2 Electron beam damage effects

Electron flood guns are used to reduce charging of insulating samples during SIMS analysis. These guns are known to cause chemical degradation of the sample surface. NPL studied the effects of electron beam damage in 3D SIMS imaging for three organic materials; Irganox 3114, NPB and poly(vinylcarbazole).

Following extensive electron beam irradiation, a damaged ellipsoidal area of 2-3 mm was identified. In depth profiles obtained with 5 keV Ar_{2000}^+ sputtering from the vicinity of the damaged area, the characteristic ion signal intensity rose from an initial low level to a steady state with increasing depth. For the damaged thin films, the ion dose required to sputter through the thin film to the substrate was higher than for undamaged areas. This was explained by the formation of a damaged layer with a sputtering yield that was reduced by up to an order of magnitude. The thickness of the damaged layer, which increased with the electron dose, was in the order of 20 nm for Irganox 3114. This effect, which was not previously recognised, shows the importance of avoiding electron beam damage for effective quantitative analysis. Optimal electron beam alignment and careful current control are essential for reducing electron beam damage. The study was reported in JASMS ([7] Havelund et al., 2014) to provide guidance for reducing damage effects.

3.2.3 Imaging of organic electronic materials

The Research Excellence Grant researcher (REG) based at IMEC visited NPL on several occasions to study sputter depth profiling of materials used in organic photovoltaic (OPV) devices. The photoactive layer in such devices is typically a bulk heterojunction of a conjugated polymer, e.g. P3HT, and a fullerene (C_{60} or C_{70}) derivative, e.g. PCBM. SIMS depth profiling holds the potential for measuring compositional variation, contaminants and degradation within the layer photoactive layer. An example of a SIMS image is shown in Figure 8. Again, the effects of E and n were studied, and the critical requirement for $E/n \leq 10$ eV observed for NPB was also found for these ionising radiation-sensitive materials.

As mentioned above, SIMS sputter depth profiling is often conducted using two ion beams in a dual-beam configuration. The ion source of choice for SIMS analysis of organics is a liquid metal ion source providing small clusters with 3 to 7 bismuth or gold atoms. Liquid metal ion sources have excellent imaging capability but induce significant damage to organic samples. In dual-beam depth profiling, this damage is continuously 'cleaned up' by the gentler large cluster ion beam. To find suitable experimental conditions the effect of the ion dose of 25 keV Bi_3^+ analysis ion beam relative to the dose of a 5 keV Ar_{2000}^+ sputter ion beam was measured. It was found that the dose ratio had to be below 0.2% to maintain characteristic ion signal intensities above 90% of the signal intensity from the pristine material. This is a useful and easily adaptable recommendation for dual-beam depth profiling of organic electronic materials.

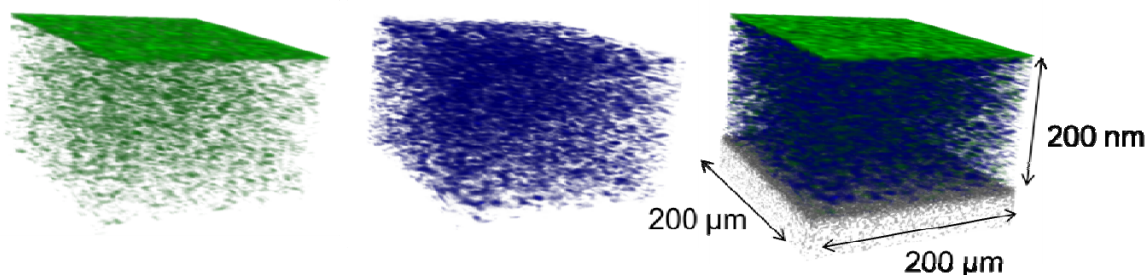


Figure 8: 3D SIMS chemical maps from a PCDTBT/PC70BM organic photovoltaic active layer. Left: PCDTBT (green), centre: PC70BM (blue) and right: overlay of the two chemical maps with the substrate shown in grey. The SIMS chemical maps reveal a polymer-enriched surface covering a mixed polymer-fullerene phase.

Quantitative analysis by SIMS is generally limited by the so-called matrix effect leading to a non-linear relationship between the analyte concentration and the secondary ion signal intensity. This relationship was investigated for the organic photovoltaic active layers through the analysis of a series of layers with known compositions. The characteristic PCBM ion signal intensity was found to be strongly enhanced by the polymer in the layers, and even be higher in some mixed layers than in a pure PCBM layer. This is a severe example of the matrix effect, and estimating the relative PCBM content based on the characteristic PCBM ion signal intensity could lead to a false result. Instead, it was found, that a calibration curve for measuring the PCBM content could be established using the ratio of the characteristic PCBM ion signal to the sum of this signal and a characteristic ion signal arising from the P3HT polymer. This important result of the collaborative research shows that SIMS can be used to quantitatively measure the composition of OPV photoactive layers and potentially provide valuable information for the optimisation of device manufacture. The work was published in *Surf Interface Anal* ([4] Fleischmann et al., 2014).

LiF is used as an electron injection layer in organic electronic devices. In such devices, the migration of Li^+ and F^- ions into the organic layers has been linked to chemical degradation leading to degrading device performance. NPL developed a bilayer model system to measure the migration of LiF into a layer of Alq3, a compound used in organic light emitting displays. SIMS depth profiles from the model systems showed two distinct layers and no signs of migration into the organic phase for temperatures up to 75°C.

3.2.4 Measuring the matrix effect in SIMS

Extending on the encouraging results for OPV materials, NPL studied the matrix effect in SIMS for two molecular mixtures. The mixed layers of Irganox 1098 with Irganox 1010 and fmoc-pentafluoro-L-phenylalanine (fmoc-PFLPA) with Irganox 1010 with compositions of 25:75, 50:50 and 75:25 were sourced from the EMRP project IND15 "Traceable quantitative surface chemical analysis for industrial applications".

SIMS depth profiles were obtained from the mixed layers and from pure material layers. When plotting the ion yields for characteristic ions for the two compounds versus the composition, a near-linear relationship was seen for some ions, however, the formation of most ions would be either suppressed or enhanced in the mixed layers relative to the pure layers. A parameter, Ξ , was introduced to describe the magnitude of the matrix effect. It was demonstrated that with some knowledge of the matrix effect magnitude and sign provided by Ξ it becomes possible to select secondary ions for reliable quantitative analysis in binary mixtures. The study also indicated how the differences in Ξ between different secondary ions may, in the future, be exploited to assess compositional variation or nanoscale phase separation in materials. A paper was published in the *International Journal of Mass Spectrometry* ([8] Shard et al., 2015).

NPL led an interlaboratory study on measuring the composition of binary layers using argon cluster sputter depth profiling under the auspices of VAMAS (Versailles Project on Advanced Materials and Standards). Layered samples with known binary compositions in each layer were manufactured in a single batch and distributed to more than 20 participating laboratories. The samples were analysed using argon cluster ion sputtering and either x-ray photoelectron spectroscopy (XPS) or SIMS to generate depth profiles.

Participants were asked to estimate the volume fractions in two of the layers and were provided with the compositions of all other layers. Participants using XPS provided volume fractions within 0.03 of the nominal values. Participants using ToF-SIMS either made no attempt, or used various methods that gave results ranging in error from 0.02 to over 0.10 in volume fraction, the latter representing a 50% relative error for a nominal volume fraction of 0.2. Error was predominantly caused by inadequacy in the ability to compensate for primary ion intensity variations and the matrix effect in SIMS.

Matrix effects appear to be more pronounced as the number of atoms in both the primary analytical ion and the secondary ion increase. Using the participants' data it was shown that organic SIMS matrix effects can be measured using the Ξ parameter and are remarkably consistent between instruments. Importantly, it was demonstrated, using a simple normalization method, that virtually all SIMS participants could have obtained estimates of the composition that were at least as accurate and consistent as XPS. Another important realization of the study was that matrix effects affect the apparent position of an interface. The results of the interlaboratory study have been summarised in a manuscript that has been published in *Journal of Physical Chemistry B* ([20] Shard et al., 2015). These studies are significant advances in quantitative SIMS analysis of organics.

3.2.5 Angle dependence of sputtering yields

Besides the energy and the cluster size, the angle of incidence is also a key parameter for argon cluster sputtering. Most commercial instruments have the argon cluster ion source at 45° to the sample surface but other configurations may be advantageous. In the project, NPL analysed the angle dependence of sputtering yields of Irganox 1010 initially using a coronene ion source. Coronene, as C₆₀, is a predecessor of argon clusters. The coronene source was found to have good behaviour at high angles of incidence with depth resolutions better than 6 nm. The sputtering yields were in agreement with the universal equation, but slightly lower than this would predict. The work was published in *J Phys Chem B* (Seah et al, 2013).

Building on this, the sputtering yields of Irganox 1010 were measured using argon gas cluster ion beams of 5 and 10 keV energy with cluster sizes from 1000 to 5000. The data showed an angular dependence of the sputtering yield with the highest yield at 45° where the yield was between 2 and 10 times that at 0°. The angle-dependence was stronger for low E/n sputtering. This was included in the Universal Equation for argon cluster sputtering yields to give a very accurate description of all the extensive Irganox 1010 data and also published experimental data from project partner ION-TOF for polystyrene. The analytical description of the behaviour, which was published in *Journal of Physical Chemistry B* ([14] Seah et al, 2015), is important for the development of the application of secondary ion mass spectrometry to organic materials.

3.2.6 Depth resolution in sputter depth profiling

The ability to discriminate between different layers in depth profiling is given by the depth resolution. To measure the depth resolution, an organic multilayer reference materials with ultrathin organic (~1 nm) layers of one material embedded in a different material is analysed. In depth profiles from this sample, the layers will appear to be wider than the actual thickness and their apparent width shows the depth resolution. NPL measured this for two different materials using argon clusters with different energies and cluster size. The depth resolution was found to improve with decreasing energy per cluster ion atom. The optimal depth resolutions in these experiments were 5-6 nm (FWHM) achieved with E/n between 1 and 2 eV, in agreement with data previously published by ION-TOF.

The incident ion angle-dependence of the depth resolution obtained at an Irganox 1010 to silicon interface was determined from depth profiling data in an x-ray photoelectron spectrometer. The results confirmed a previously published relation for the depth resolution with the sputtering yield, roughly $FWHM = 2.1 Y^{1/3}$. The relation is valid both at the 45° incidence angle of the argon gas cluster sputtering ions used in most studies and at all angles from 0° to 80°. This would indicate that, for optimal depth profile resolution, 0° or greater than 75° incidence would be significantly better than the 45° traditionally used, especially for the low E/n settings used for the most detailed argon gas cluster depth profiles of organic materials due to the low sputtering yield at these angles. A more detailed analysis, however, showed that there were minimal

improvements at 0° or greater than 75° , and this was confirmed by a critical test on a delta layer in SIMS at 75° . The work has been published in the journal *Analyst* ([19] Seah et al, 2015) and provides guidance for analysts to select E and n for practical analysis.

3.3 3D nano-electrical and optical characterisation of organic semiconductor nanostructures

Mapping of electrical and photo-electrical properties on the nanoscale using atomic force microscopy (AFM) and photoconductive AFM (PC-AFM) provides a means for directly measuring the properties and mechanisms that govern the performance of organic electronic devices. The project aimed to improve the applicability and reliability of PC-AFM and to develop a novel simulation tool to extract 3D nano-electrical information from the measurement data. To support these developments, micro- and nano-structured reference materials were required. In addition to the electrical characterisation, optical characterisation by spectroscopic ellipsometry was investigated for quantitative, non-destructive characterisation of organic layers.

3.3.1 Development of nanostructured self-assembled reference materials

Nanostructured reference materials are required for the development of nano-analytical techniques. In the project, a number of materials and nanostructured systems were used to fabricate model samples with features in the range from 10 to 200 nanometers for photoconductive AFM. Regular model structures based on diblock copolymers PS-*b*-PMMA with a pitch of 17 nm, a height of 30 nm, and with FIB “find me structures” were delivered to REG(IMEC) for deposition of OPV materials on these structures. A second sample system with microstructures in a conductive ITO film were sent to NPL for PC-AFM characterization. A third group of samples consisting of OPV active layer materials were fabricated by IMEC.

FIB preparation and SEM, Bright Field TEM and STEM analyses were successfully carried out on the model samples as fabricated and after impregnation with organic material. For the analyses, two lamellas were cut, extracted and manipulated by standard lift-out technique from the samples delivered to NPL.

SEM and STEM analysis was performed with a FEI Quanta 3D DualBeam ESEM FEG at Nanofacility Piemonte INRiM, and TEM and (S)TEM analysis was performed at the FEI Nanoport Eindhoven using a FEI Titan™ Themis3 300 with two spherical aberration correctors and a Talos F200X.

The fabrication process based on diblock copolymers is more controllable than self-assembly of nanospheres to form regular structures. A systematic study of the self-assembly of asymmetric polystyrene-*b*-poly(methyl methacrylate) (PS-*b*-PMMA) block copolymer-based nanoporous thin films over a broad range of molar mass (M_n) between $39 \text{ kg} \cdot \text{mol}^{-1}$ and $205 \text{ kg} \cdot \text{mol}^{-1}$ was performed. We demonstrated that a fine tuning of the annealing parameters, performed by a Rapid Thermal Processing (RTP) machine, allows to obtain an almost continuous variation of lattice parameters. This is achieved by varying M_n and changing the annealing temperature, whilst keeping the annealing time (900 s), the film thickness ($\sim 30 \text{ nm}$), and the PS fraction (~ 0.7) constant. The morphology, the characteristic dimensions (i.e., the pore diameter, d , and the pore-to-pore distance, L_0), and the order parameter (i.e. the lattice correlation length, ξ) of the samples were analysed using scanning electron microscopy and grazing-incidence small-angle X-ray scattering (see Figure 9). The obtained values of d were between 12 and 30 nm, and L_0 between 24 and 73 nm (Table 2). The results evidence the capability to tailor the self-assembly processes of block copolymers over a wide range of molecular weights by a simple thermal process to achieve structures that are fully compatible with the stringent constraints of metrology, lithographic applications and industrial manufacturing. This study led to the publication of two papers in high impact factor journals ([12] Perego et al., 2014 and [15] Ceresoli et al., 2014)

Table 2. Preparation and morphological parameters of optimized BCP samples: Film thickness h (measured by ellipsometry), annealing temperature T_A , χN values calculated at $T = T_A$, cylinder diameter d (measured by SEM), lattice spacing measured by SEM $L_{0\text{SEM}}$ and by GISAXS $L_{0\text{GISAXS}}$, and correlation length ξ (measured by GISAXS)

sample	h (nm)	T_A (°C)	χN (at T_A)	d (nm)	L_{0SEM} (nm)	$L_{0GISAXS}$ (nm)	h/L_0	ξ (nm)	ξ/L_0
B39	33	180	13.8	12.0 ± 2.0	26.0 ± 1.0	23.5 ± 0.2	1.37	447	19
B54	29	200	18.0	13.0 ± 1.0	28.8 ± 0.5	28.3 ± 0.3	1.00	477	17
B67	27	250	23.1	17.0 ± 1.0	35.0 ± 1.0	34.4 ± 0.4	0.77	710	21
B82	34	250	28.2	19.0 ± 2.0	42.9 ± 0.7	43.9 ± 0.7	0.79	535	12
B102	33	230	35.5	22.7 ± 1.5	47.0 ± 1.0	48.7 ± 0.9	0.70	434	9
B132	28	240	45.6	28.6 ± 1.6	59.0 ± 4.0	62.1 ± 1.4	0.47	354	6
B205	35	240	70.9	30.0 ± 4.0	75.0 ± 8.0	74.0 ± 2.0	0.48	357	5

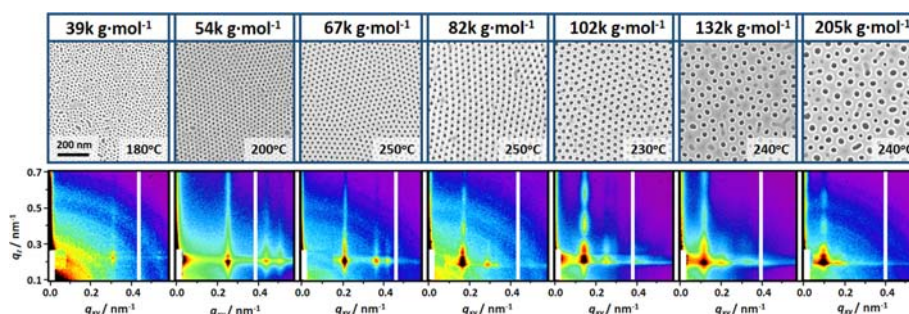


Figure 9: SEM images and corresponding GISAXS patterns for PS-b-PMMA thin films of increasing M_n after removal of PMMA domains. The corresponding annealing temperatures are also reported. All GISAXS patterns have been recorded at an incidence angle $\alpha_i = 0.18^\circ$, except the B39 where $\alpha_i = 0.15^\circ$.

Based on the molar mass study above, the B67 copolymer was chosen as a model sample system for PC-AFM studies. A lamella from this sample was prepared with the Quanta 3D Dualbeam system at INRiM and investigated at the FEI Nanoport. In Figure 11 (left), the bright-field TEM image of the section after C_{60} deposition, and (right) STEM HAADF EELS spectra recorded along the vertical green line at different positions of the self-assembled block copolymer layer covered with the OPV materials. From spectrum 1 to 5, shown in the inset, the carbon peak slightly increases, revealing a transition from a polystyrene-rich structure to the complete C_{60} phase.

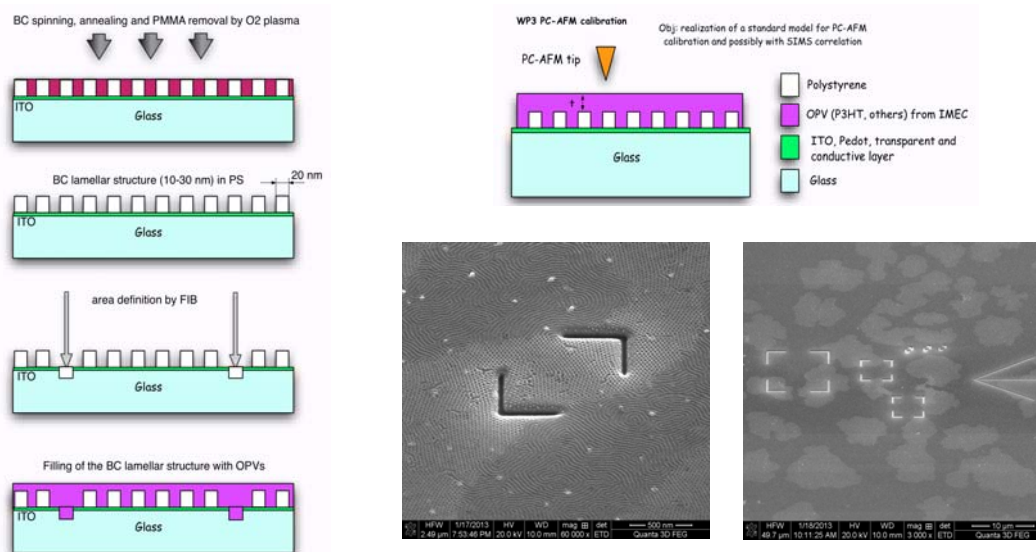


Figure 10: Left: process scheme for diblock copolymers self-assembly on ITO and C_{60} deposition, upper right: final configuration scheme. Lower right: SEM micrographs of the final sample models (before C_{60} deposition),

based on B67 diblock copolymer (horizontal and vertical cylinders of 17.0 ± 1.0 nm) and 10, 5 and 1 micrometers FIB “Find me” structures defined by FIB

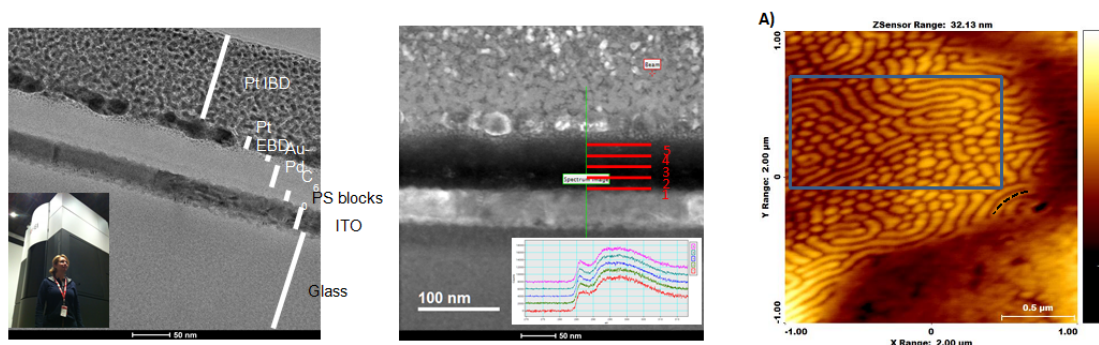


Figure 11: Left: bright field section of the sample model after C60 deposition. In the inset the Titan TEM at FEI. Center: STEM HAADF EELS spectra recorded along the vertical green line in points of the self-assembled BC layer covered with OPV. From spectrum 1 to 5, the Carbon peak slightly increases, revealing a transition from a polystyrene-rich structure to a complete C60 phase. Right: Representative topography image of the diblock copolymer+C60 sample on ITO by PC-AFM. Boxed region was used for the roughness analysis, where the area $R_a = 1.6$ nm. Clearly a two phase system is observed, which is in agreement with the SEM images provided by INRIM. An amorphous region surrounds the lamella region, with a typical $R_a = 1.1$ nm.

For PC-AFM an alternative approach in which physical holes were created in the ITO layer directly (see Figure 11) was also developed. Holes with increasing dimensions were created at INRIM. These were sent to IMEC for coating with 120 nm of C60 and then sent to NPL for conductive AFM measurements (Figure 12). The holes can be clearly seen in both topography and conductive AFM data. The advantage of the ITO hole samples is that almost any thin film material can be deposited onto the reference holes and it can potentially be used more than once if the layer is removed by wet etching. On the other hand, the PS samples represent the advantage of being much simpler and cheaper to fabricate at the same time as being well suited to act as a reference material for dimensional measurements at the nanoscale.

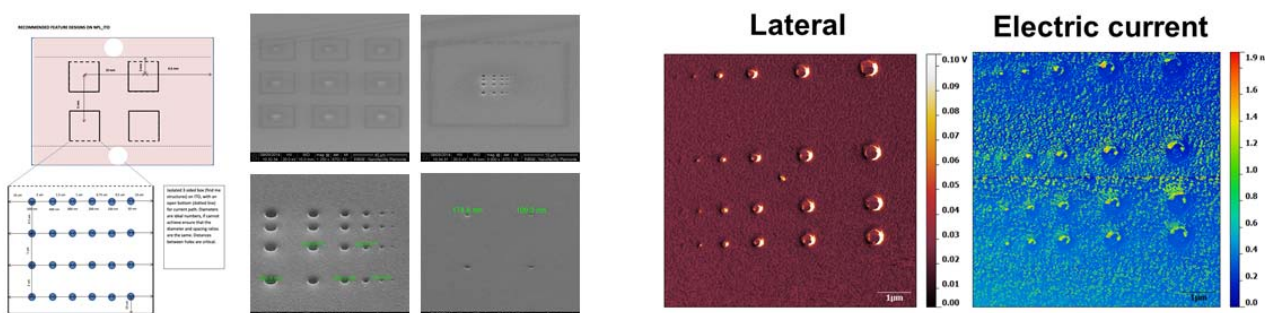


Figure 12: Left: layout and SEM microphotographs of the samples obtained by FIB patterning approach directly onto ITO. Right: Topography (left) and electrical current (right) measurements of a reference sample with FIB produced holes in ITO film on glass coated with 120 nm of C60. Samples prepared by INRIM (holes) and IMEC (C60 coating) and measured by NPL.

3.3.2 Optical characterization of organic photovoltaic materials

Two-component ultra-thin film blends are used as the active layer in organic photovoltaic devices. OPVs consisting of conjugated polymers and fullerene derivatives receive increasing attention due to relative ease of preparation, low cost and high power conversion efficiency. BAM analysed a blend of the polymer PCDTBT and the fullerene derivative PC₇₀BM (with the concentration of fullerene ranging from 50% to 95%)

produced by spin coating on thermally oxidized Si substrates covered with a thin layer of MoO₃ by IMEC. As the internal distribution of the components strongly determines device performance, an extensive study involving spectroscopic ellipsometry, atomic force microscopy and TOF-SIMS techniques was performed to understand the composition and structure of the investigated samples (above, Figure 8). Two important results were obtained from atomic force microscopy studies and further used for the ellipsometric theoretical modelling: 1) the samples with a high PC₇₀BM concentration show smoother surfaces, 2) no obvious phase separation was observed, which points to a finely mixed morphology at the surface of the samples.

The main goal of this activity was to develop fast, non-destructive and contact-less characterization methods to study the vertical distribution in the blends. Spectroscopic ellipsometry in the wavelength range 350 nm to 1670 nm was employed to determine the thickness of the studied layers, the optical constants of the pristine components as well as the mixed layers, the fullerene derivative concentration in the mixture and to detect vertical phase separation. The refractive index and extinction coefficient were calculated by considering an effective medium approximation model and are presented in Figure 13. The fingerprints of the two pristine constituents can be identified in the optical constants of the blends.

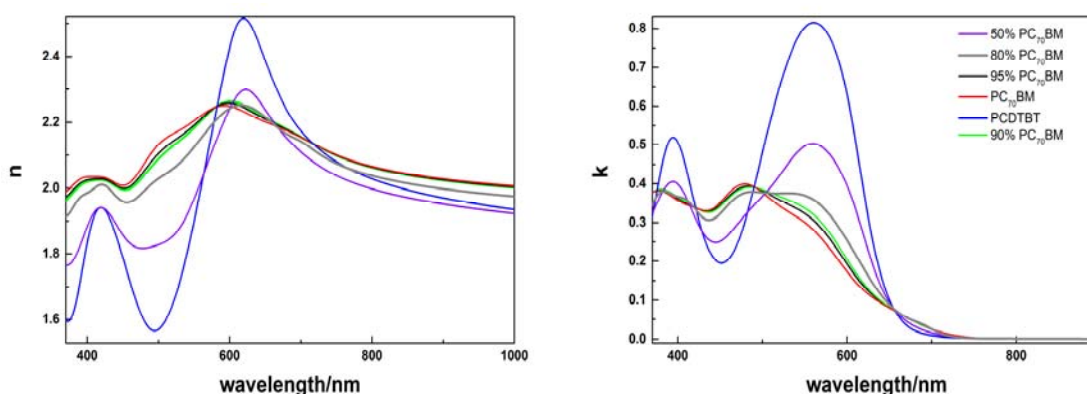


Figure 13: Optical constant of different PCDTBT / PC₇₀BM blends determined by goniospectral ellipsometry.

A clear difference can be noticed for different fullerene concentrations. A considerable reduction of the absorption with increasing the PC₇₀BM concentration was observed above 500 nm as well as a slight shift in the position of the bands, which might be an indicator of a change in the crystallinity of the polymer in the blend. Important to mention here is the fact that for all above investigations, a homogeneous distribution of the two phases (constituents) in the blend was considered; a vertical phase separation could not be established. NPL confirmed the homogeneity of the blended layers, apart from a polymer-rich overlayer, by employing TOF-SIMS measurements on two of the investigated samples (Figure 8).

This is the first time this type of analysis has been demonstrated on OPV samples with an analysis model involving the effective medium approach and confirmed by ToF-SIMS depth profiling. The result is an important step towards establishing optical methods as process control tools while maintaining traceability.

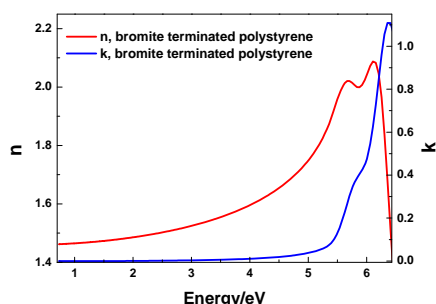
3.3.3 Evaluation of toluene content in polystyrene nanolayers

From studies carried out in the framework of the project, it was found that residual solvent plays a primary role in the self-assembly of diblock copolymer systems. Monitoring the evolution of toluene, before and after the annealing and segregation is key to deliver more controlled morphologies and model systems at the sub-50 nm scale. For this purpose, a set of polystyrene layers on silicon prepared at INRiM were measured by spectroscopic ellipsometry. The samples were grafted and thermally annealed, then spin coated with anionic polystyrene layers of different thickness and toluene content.

BAM investigated the samples using spectroscopic ellipsometry in the range 0.7-6.5 eV. Measurements with the angle of incidence between 45° and 75° (step 2.5°) were performed in order to ensure a sufficient set of data for the determination of the desired parameters. The thickness of the native oxide of the substrates was

determined using spectroscopic ellipsometry with a two-layer model. Using the optical constants for silicon oxide found in the literature, the determined oxide thickness was 1.27 nm.

The thickness and the refractive index of the thermally treated polystyrene were obtained using a dispersion model in the transparent spectral range. 8.75 nm and a refractive index of 1.455 are reported. For the determination of the optical constants of the layer, a three-layer model was considered (Si, SiO₂ and a layer described by an oscillator model). The oscillator layer is described by using one Gauss oscillator and one Lorentz oscillator. The optical constants are presented in Figure 14.



Sample	Thickness (nm)	Residual solvent (%)
HE07	62.8	23.0
HE08	38.3	24.4
HE09	26.9	26.6

Figure 14: Optical constants of one of the grafted PS sample. **Table 3:** Right: PS nanolayers samples and relative toluene content evaluated by ellipsometry and by mass spectrometry.

By ellipsometry, it is possible to determine the thickness and the solvent content of these layers in the same experiment. An effective medium approximation model with two constituents was considered in the spectral range [0.7–4.5] eV. One of the constituents was described by the optical constants described in the previous paragraph, the second was a Cauchy layer used to describe the residual solvent. In order to reduce the correlation between the parameters, a multi-sample analysis was employed. Table 3 summarizes the calculated parameters. The residual solvent amounts found by BAM in the samples are in good agreement with the amount of toluene previously determined in a similar system. In fact a $26.2 \pm 0.3\%$ of toluene was found in a two layer system constituted by a grafted layer of P(S-r-PMMA) on which a second layer of an symmetric PS-b-PMMA block copolymer was spin coated.

3.3.4 Development of a novel method for 3D nano-electrical characterisation of organic semiconductor nanostructures

This project has demonstrated a novel method for 3D nano-electrical characterisation of organic semiconductor nanostructures with resolution below 30 nm. The approach is based on electrical atomic force microscopy (AFM) and quasi-3D characterisation of organic semiconductor nanostructures. We focused on two steps to achieve the objective above: development of reliable 2D mapping method and development of a novel simulation tools to extract 3D nano-electrical information from the measurement data.

(Photo)conductive AFM was the method of choice for this work. In these measurements a conductive probe, typically metal-coated Si, is used in contact with the sample of interest to measure the current flowing from (or to) the substrate. By scanning the probe over the surface a 2D image of the (photo)current can be obtained with the lateral resolution limited by the contact area between the probe apex and the sample. As this current travels through the organic thin film, both surface and subsurface information can be obtained. The main challenge however is to distinguish between these two sources of information and understand the subsurface image, i.e. to know the depth of the features observed.

In order to solve these challenges, the project focused on investigating the main sources of uncertainty in photoconductive AFM and developing modelling and experimental methods to probe the subsurface information. The project tackled the main sources of uncertainty by developing a reliable measurement protocol and putting in place engineering control actions to minimise these sources of uncertainty. That

included the use of high quality nitrogen gas and calibrated mass flow controllers to avoid sample degradation without inducing mechanical noise; temperature stabilisation; laser spatial homogeneity and laser power stability; good definition of sample-probe contact area. The latter is possibly the most significant source of uncertainty in any AFM measurement. In particular for electrical measurements, changes in tip shape during measurements can introduce image artefacts and make quantification almost impossible. There is no simple way to measure the contact area for electrical AFM, which can differ from the dimensional area, therefore one of the aims of this project was to develop reference samples that could reduce the uncertainties in estimating this parameter.

In order to build a better understanding of the results from such analyses and the impact of different measurement parameters on the reliability of the method, NPL and CMI developed modelling methods and software to simulate the full experiments. Two approaches were developed. One was focused on measurements on organic semiconductor thin film solar cells and is based on a master-equation solution of a three-dimensional hopping charge transport model which includes donor-acceptor domain morphology, energetic and spatial disorder, exciton transport and splitting, charge-pair generation and recombination, and tip-substrate electrostatics ([16] Blakesley and Castro, 2015). A novel simplifying aspect of the model is that electron transport, hole transport and electron-hole recombination are treated as the same electron-transfer process. The model recreates realistic bulk recombination rates, without requiring short-range Coulombic effects to be calculated. It also shows a loss in resolution as the imaged feature moves from the surface to inside the film (Figure 15a), similar to feature broadening observed in experimental results. This allows to probe 3D information within the 2D images.

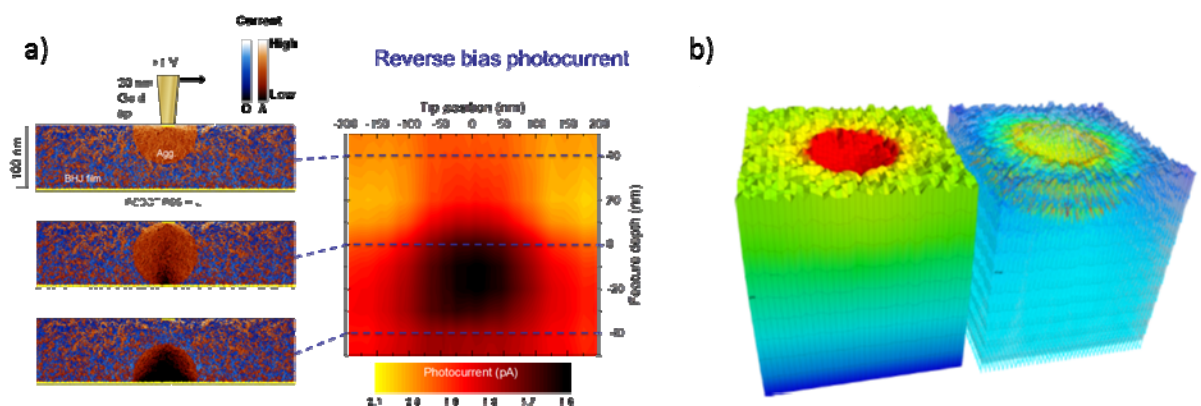


Figure 15: a) Simulated photocurrent line scans of 100 nm-diameter acceptor clusters at various depths within an organic solar cell under reverse bias and ~ 10 Sun irradiance. left) Film cross-sections showing current hotspots for clusters at three different depths. Blue spots are donor sites and red are acceptor sites. Lighter colour corresponds to higher currents. right) A current image constructed by assembling line scans for clusters at different depths. A feature depth of +50 nm corresponds to the cluster's centre being on the surface of the film. b) Simulated indentation into randomly generated rough surface and a computation of electrical current coming from the probe into the sample.

The second approach was focused on measurements on inorganic thin films composed of nano clusters of Si crystals on amorphous Si and is based on a combination of a Finite Difference in Time Domain method for optical calculations and a hopping transport model for electron transport treatment. The effect of sample elastic deformation due to the tip on the measured electric current was investigated (Figure 15b) and the software allows for sample deformation to be included during the simulation of the complete PC-AFM measurement. However, the calculation of deformation adds significant computational cost which limits its application to highly specific and simplified experiments. Nevertheless, we developed and demonstrated a complete model that can be used to estimate resolution, topography related artefacts that are sources of large uncertainties in electrical AFM experiments.

The modelling tools give a better understanding of the 3D information contained in the experimental 2D images obtained by PC-AFM measurements and will allow future work on new methods to directly measure 3D information.

4 Actual and potential impact

The project has delivered a high scientific output. To obtain a long term sustainable impact in the scientific community the communication channels of written manuscripts, presentations and training at conferences were chosen. The key data of the project are the following:

- 20 publications in the public domain and another 6 publications anticipated
- 66 conference presentations and posters
- 12 training sessions

The consortium organised several special sessions and workshops including a highly successful European Materials Research Society Symposium continuing the ALTECH conference series. In total 160 contributions were presented, including 11 invited presentations, 87 contributed oral presentations and 69 poster presentations.

Throughout the project, the partners engaged in pre-normative and standardisation activities in VAMAS (Versailles Project on Advanced Materials and Standards) and under ISO, as well as the national bodies DIN (Germany) and BSI (UK). Based on results from the project, NPL led the discussion on a standard for sputter depth profiling of organic materials at the ISO/TC201 (Surface Analysis) meeting in Berlin, September 2014. The development of a standard was encouraged by the committee.

The improved capability of reference-free GIXRF to quantify low mass depositions of a high variety of elements, including high-k dielectric materials on various substrate materials, is the prerequisite for (fundamental) studies aiming at a detailed understanding of deposition processes, reaction mechanisms and origins of growth inhibition in nanoelectronics manufacture. In addition to its fundamental importance, the reference-free quantification method is also of high relevance in process technology and layer engineering, where quantification of various materials is performed on a routine basis relying on calibration standards. The reference-free GIXRF method allows for the qualification of calibration standards used for laboratory equipment or to perform a reliable quantification of unconventional materials. This quantification approach reduces the dependency on appropriate reference materials, which are rarely available for nanolayered systems and enables the qualification of calibration standards for inline TXRF analysis.

Argon cluster sources have become highly popular. Today, more than half of new SIMS and x-ray photoelectron spectroscopy instruments are sold with an argon cluster source. An estimated >200 are now in operation worldwide in industry and academia and several measurement service providers offer depth profiling of organic electronic devices. Companies in the organic electronics industry regularly make use of these to assess layer and interface chemistry, for example to locate and identify contaminants that compromise device performance. The rapid uptake of argon cluster sources creates an increased need for robust measurement procedures. The outputs of the project comprise a timely response to this need. Analysts can now rely on the extensive body of work generated in the project that will help them select appropriate analytical conditions for optimal analytical capability and reliability. The immediate uptake of the results is evident from the project's 10 scientific publications in this area having been cited more than 80 times in the scientific literature in total as at February 2016. To accelerate the uptake of the outputs in industry, a follow-on project has been established in the EURAMET EMPIR programme to convey the results into an international standard for argon cluster depth profiling. The development of this standard was encouraged by stakeholders from industry and the metrology community. Its availability is envisaged to ensure reliable chemical depth profiling to underpin and accelerate innovation in the organic electronics industry, contributing to economic growth and development of environmentally friendly and low cost technologies.

The universal equation for cluster sputtering has led to a new route to clean graphene surfaces to prepare the graphene for chemical modification and incorporation into novel electronic devices (Tyler et al, *J Phys Chem C*, 2015). This research shows that polymer residues left from the transfer process in single layer graphene production may be sputtered away using argon clusters whilst leaving the graphene virtually undamaged. With the great potential graphene-technologies hold, in particular due to the extraordinary electric properties, this could have important commercial application and is especially useful since it is already compatible with the current 300 mm semiconductor production standard.

Advanced software has been developed in this project to allow simulation of the impact of nanoscale 3D morphology on the measurement of electrical properties with resolution below 30 nm. This will support the development of nanoscale electrical measurements to directly assess key properties for organic photovoltaic devices and so underpin growth in the nanoelectronics industry.

Our research has also had far greater impact in fields previously not envisaged in this research. For example, the pharmaceutical industry has taken up the results of our research to use 3D SIMS imaging to measure the drug disposition in tissue and cells. This has led to ION-TOF GmbH (member of this consortium) and Thermo Scientific (not in this consortium) to invest in building a revolutionary new instrument - the 3D nanoSIMS (see press release <http://www.npl.co.uk/news/3d-nanosims-label-free-molecular-imaging>). Sir Colin Dollery adviser to the GlaxoSmithKline Chairman of Research and Development comments: "GlaxoSmithKline scientists are looking forward to the opportunities the new equipment will provide to explore in detail the sites of action of novel drug molecules within single cells. Designing drugs that are specific for molecular targets is part of drug development but knowing that they reach their target molecule in the right amount at the right place in the right cells is only just beginning to be attainable in intact cells within tissues. This ability will be a great opportunity."

5 Website address and contact details

Project website: <http://projects.npl.co.uk/NEW01-TReND/>

Contact (technical lead):

Prof. Ian S Gilmore
National Physical Laboratory
Hampton Road, Teddington
TW11 0LW,
United Kingdom
Email: ian.gilmore@npl.co.uk
Tel: +44 (0)20 8943 6922

6 List of publications

1. Sputtering Yields for Gold Using Argon Gas Cluster Ion Beams. L. Yang, M. P. Seah, and I. S. Gilmore, *J Phys Chem C*, 2012, 116, 23735-23741
2. Depth Profiling and Melting of Nanoparticles in Secondary Ion Mass Spectrometry (SIMS). L. Yang, M. P Seah, I. S Gilmore, R.J.H. Morris, M. G. Dowsett, L. Boarino, K. Sparnacci, and M. Laus, *J. Phys. Chem. C*, 2013, 117, 31, 16042-16052.
3. Universal Equation for Argon Gas Cluster Sputtering Yields. M.P. Seah, *J. Phys. Chem. C*, 2013, 117 (24), 12622–12632.

4. Fundamental aspects of Arⁿ⁺ SIMS profiling of common organic semiconductors. C. Fleischmann, T. Conard, R. Havelund, A. Franquet, C. Poleunis, E. Voroshazi, A. Delcorte and W. Vandervorst, *Surface and Interface Analysis*, 2014, 1 (46), 54-57.
5. G-SIMS analysis of organic solar cell materials. A. Franquet, C. Fleischmann, T. Conard, E. Voroshazi, C. Poleunis, R. Havelund, A. Delcorte and W. Vandervorst, *Surface and Interface Analysis*, 2014, 1, (46), 96-99.
6. SIMS of organics—Advances in 2D and 3D imaging and future outlook. I. S. Gilmore, *J. Vac. Sci. Technol. A*, 2013, 31, 050819.
7. Electron Flood Gun Damage Effects in 3D Secondary Ion Mass Spectrometry Imaging of Organics. R. Havelund, M.P. Seah, A.G. Shard, I.S. Gilmore, *J Am Soc Mass Spectrom.*, 2014, 25 (9), 1565-71.
8. The matrix effect in organic secondary ion mass spectrometry. A.G. Shard, S.J. Spencer, S.A. Smith, R. Havelund, I.S. Gilmore, *International Journal of Mass Spectrometry*, 2015, 377 (1), 599-609.
9. Universal Equation for Argon Cluster Size-Dependence of Secondary Ion Spectra in SIMS of Organic Materials. M.P. Seah, R. Havelund, I.S. Gilmore, *J. Phys. Chem. C*, 2014, 118 (24), 12862–12872.
10. Characterization of high-k nanolayers by grazing incidence X-ray spectrometry. M. Müller, P. Hönicke, B. Detlefs, C. Fleischmann, *Materials*, 2014, 7(4), 3147-3159.
11. Characterization of Semiconductor Samples using Synchrotron Radiation-based Near-Field Infrared Microscopy and nano-FTIR Spectroscopy. P. Hermann, A. Hoehl, G. Ulrich, C. Fleischmann, A. Hermelink, B. Kästner, P. Patoka, A. Hornemann, B. Beckhoff, E. Rühl, and G. Ulm. *Optics Express*, 2014, 22 (15), 17948-17958.
12. Ordering Dynamics in Symmetric PS-b-PMMA Diblock Copolymer Thin Films During Rapid Thermal Processing. M. Perego, F. Ferrarese Lupi, M. Ceresoli, T. J. Giammaria, G. Seguini, E. Enrico, L. Boarino, D. Antonioli, V. Gianotti, K. Sparnacci, M. Laus, *J. Mater. Chem. C*, 2014, 2, 6655-6664.
13. Reference-free, depth dependent characterization of nanoscaled systems with advanced grazing incidence X-ray fluorescence analysis. P. Hönicke, M. Müller, B. Detlefs, C. Fleischmann, B. Pollakowski, B. Beckhoff, *pss(a) - ALTECH Proc*, 2015, 212 (3) 523-528.
14. Angle Dependence of Argon Gas Cluster Sputtering Yields for Organic Materials. M. P. Seah, S. J. Spencer, A.G. Shard, *J. Phys. Chem. B*, 2015, DOI: 10.1021/jp512379k.
15. Evolution of lateral ordering in symmetric block copolymer thin films upon rapid thermal processing. M. Ceresoli, F. Ferrarese Lupi, G. Seguini, K. Sparnacci, V. Gianotti, D. Antonioli, M. Laus, L. Boarino, M. Perego, *Nanotechnology*, 2014, 25 (27), 275601.
16. Simulating photoconductive atomic-force microscopy on disordered photovoltaic materials. J.C. Blakesley, F.A. Castro, *Phys Rev B*, 2015, 91, 144202.
17. Fundamental parameters of Zr and Ti for a reliable quantitative X-ray fluorescence analysis, M. Kolbe, P. Hönicke, *X-ray spectrometry*, 2015, 44 (4), 217 – 220
18. Sampling Depths, Depth Shifts, and Depth Resolutions for Bin⁺ Ion Analysis in Argon Gas Cluster Depth Profiles. R. Havelund, M.P. Seah, I.S. Gilmore, *J Phys Chem B*, 2016.

19. Depth resolution at organic interfaces sputtered by argon gas cluster ions: the effect of energy, angle and cluster size. M. P. Seah, S. J. Spencer, R. Havelund, I. S. Gilmore and A. G. Shard, *Analyst*, 2015
20. Measuring Compositions in Organic Depth Profiling: Results from a VAMAS Interlaboratory Study. A. G. Shard, R Havelund, S. J. Spencer, I. S. Gilmore, M. R. Alexander, T. B. Angerer, S. Aoyagi, J-P Barnes, A. Benayad, A. Bernasik, G Ceccone, J. D. P. Counsell, C. Deeks, J. S. Fletcher, D. J. Graham, C. Heuser, T. G. Lee, C. Marie, M. M. Marzec, G. Mishra, D. Rading, O. Renault, D. J. Scurr, H. Shon, V. Spampinato, H Tian, F. Wang, N. Winograd, K. Wu, A. Wucher, Y. Zhou, and Z. Zhu. *J. Phys Chem B*, 2015

Furthermore, six publications are under preparation, covering

21. Comparison of lab-based and synchrotron-based quantification of Al in thin ALD Al₂O₃ films (CEA and PTB).
22. Depth profiling of thin TiN layers by GIXRF (CEA and PTB).
23. Amorphous Gadolinium Aluminate as a Dielectric and Sulfur for Indium Phosphide Passivation (IMEC, PTB).
24. Inorganic material profiling using Arn + cluster: Can we achieve high Quality profiles? (IMEC, NPL).
25. Basic interactions during inorganic materials profiling with oxygen cluster beams (IMEC, ION-TOF).
26. Formation of nanostructures during relaxation of strained GeSn thin films (IMEC, PTB).